

Minutiae-Based Fingerprint Identification Using Gabor Wavelets and CNN Architecture

Pelin Görgel^{ID}, Abdulsamet Ekşi^{ID}

Department of Computer Engineering, İstanbul University-Cerrahpaşa, Faculty of Engineering, İstanbul, Turkey

Cite this article as: Görgel P, Ekşi A. "Minutiae-based Fingerprint Identification using Gabor Wavelets and CNN Architecture," *Electrica*. vol. 21, no. 3, pp. 480-490, Sep. 2021.

ABSTRACT

Fingerprint identification is still a challenging issue for confident authentication. In this study, we present a methodology that comprises pre-processing, minutiae detection, and Gabor wavelet transform. Both Gabor wavelet and minutiae features, such as ridge bifurcation and ending enhancement, represent the significant information belonging to fingerprint images. Pre-processing algorithm affects minutiae extraction performance. So we use the dilation morphological operation and thinning for the enhancement. Then Gabor wavelet transform is applied to minutiae-extracted images to increase the identification performance. The classification problem is solved using a proper convolutional neural network (CNN) with a three-layer convolutional model and appropriate filter sizes. Experimental results demonstrate that the classification accuracy is 91.50% and the proposed approach can achieve good results even with poor quality images.

Index Terms—Biometric image processing, convolutional neural network (CNN), Gabor wavelet transform

Corresponding Author:

Pelin Görgel

E-mail: pelin.gorgel@iuc.edu.tr

Received: June 7, 2021

Accepted: August 4, 2021

Available Online Date: August 27, 2021

DOI: 10.5152/electr.2021.21065



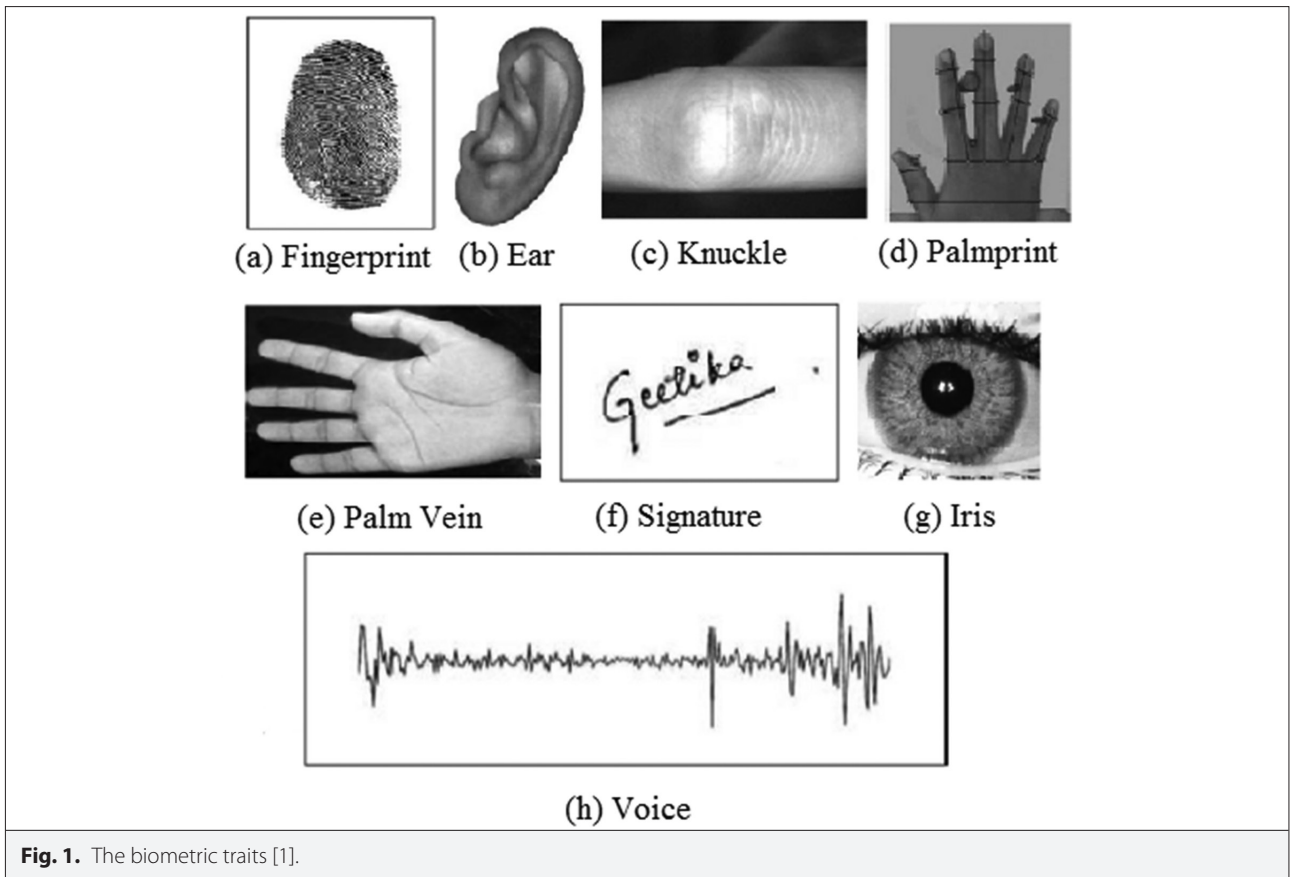
Content of this journal is licensed under a Creative Commons Attribution-NonCommercial 4.0 International License.

I. INTRODUCTION

In our electronically interconnected society, the usage of biometrics is an evolving area in recognition, and a verification system is essential in many sectors of our life especially in security and criminal identification. Furthermore, fingerprint recognition has been widely used in e-banking, e-commerce, and access control applications. The main reason is that acquiring fingerprints is easy via a fingerprint reader. The traditional authentication tools such as passports, identity cards, and passwords are well accepted in the world but they are prone to steal or forge easily. The physiological biometrics involving fingerprint, face, iris, voice, hand geometry, knuckle, palm print, is an alternative to the traditional identification systems (Fig. 1) [1,2]. The biometric system relies on the fact that every individual is different in terms of physical and behavioral aspects in various ways. Because biometric identifiers are different in every individual, they are considered permanent and unique [3].

Several approaches have been implemented so far related to fingerprint identification that compares the given fingerprint input with the existing central fingerprint templates in the database. A fingerprint comprises ridges and valleys on the fingertip surface. Most fingerprint matching systems process on gray-scale images, phase images, skeleton images, and minutiae which represent the ridge ending and ridge bifurcation. A ridge ending is a point where a ridge ends suddenly and a ridge bifurcation is a divergent point of a ridge into branch ridges (Fig. 2) [4].

Puertas et al. [5] provided manual and automatic minutiae extraction for fingerprints both with latent, rolled, and plain types. Zhang et al. [6] used a fixed image size of different resolutions (from 500 to 2000 dpi) with minutiae and pores features which are the two most beneficial fingerprint features. Ezeobiejesi and Bhanu [7] proposed a deep neural network-based fingerprint image segmentation using Restricted Boltzmann machine. They combined unsupervised learning, fine-tuning, and gradients.



The studies [8–10] utilized texture-based indexing methods to prepare a feature set including ridge orientation and frequency, ridge pattern types, ridge core, flow, and delta structure. In [9], polar complex moments were used to construct feature vectors. Then rotation invariant fingerprint representation was implemented using FVC2002 and NIST DB4 databases. The feature set was combined with minutiae and ridge frequency to increase the system performance. Global features were not enough to handle distortions like occlusion, translation, rotation, scale, etc. Anand and Kanhangad [10] used Delaunay triangulation to extract the features related to fingerprint pores. The feature vectors were then classified by an unsupervised k-means algorithm with Euclidean distance. The studies

[11–15] utilized minutiae-based indexing methods. According to these studies minutiae-based approaches achieve higher accuracy due to offering more efficient information than ridge frequency and orientation provided. In [12] minutiae was used with geometric hashing which consisted of indexing and linear time complexity searching. Then they constructed feature vectors called minutia binary patterns. Each vector was stored in a hash table exactly to reduce the computational cost. In the study of Tiwari and Gupta [11], fixed-length feature vectors representing each minutia called coaxial gaussian track code indexing scheme were constructed. Feature vectors were stored in a quantized lookup table which did not require rehashing due to well-distributed minutiae. Jin et al. [13]

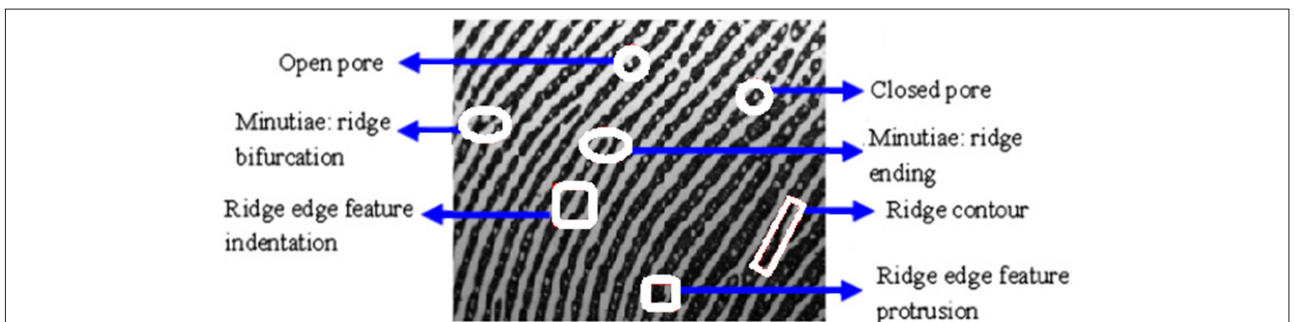


Fig. 2. Fingerprint basic features [4].

utilized the distance between the points, the difference between their angles, and the two angles between points orientation and the line joining them. Also in Wang and Hu [14] feature vectors that were alignment-free and non-invertible were extracted from minutiae pair using densely infinite-to-one mapping.

Recently deep learning methods have been used for biometric systems [1]. A deep learning topology represents data using a series of algorithms to solve classification and prediction fingerprint identification. Deep learning achieves high performance in supervised learning by extracting identical features from the dataset. It requires a large amount of training data to deal with the complexity and biometric noise. Convolutional neural network (CNN), long short-term memory, deep belief network, recurrent neural network, gated recurrent unit, and deep stacking network are counted as deep learning architectures [3]. Cao and Jain [16] proposed a system based on CNN and aligned the fingerprints in an orientation field dictionary. The trained CNN model's last fully connected layer produced a fixed-length feature vector. After then they developed another fingerprint identification methodology [17] using minutiae templates and Gabor filters. They used ConvNets to train the system which outputs a 128-dimensional feature vector and graph matching algorithms to calculate similarity scores. In Bai et al., [18] real-valued minutia cylinder code (MCC) was given to the network as inputs and binary MCC was produced as outputs. Binary MCC was used as hash table addresses to increase the search speed.

The aim of this work is to propose a minutiae-based fingerprint identification using Gabor wavelet transform (GWT) and CNN architecture. The main contributions are: i) Developing an effective minutiae extraction algorithm that detects the ridge edges and bifurcations; ii) deriving the mean of GWT in four angles from minutiae extracted images to get the significant data more comprehensively; and iii) constructing an effective CNN model with various filters and layers to reach a higher fingerprint identification accuracy. The paper is organized as follows: Section II presents the materials and methods of the proposed work, Section III provides the experimental results in terms of the performance metrics, and finally Section IV describes the conclusion.

II. MATERIALS AND METHODS

A. Proposed Work

The fingerprint images taken from the FVC2006 database [19] were passed through enhancement and thinning processes consecutively. Then minutiae extraction and GWT methods were applied sequentially to the thinned images. Finally, the derived features were given to a CNN machine learning architecture. Fig. 3 demonstrates the flow in the training and testing phases. In a fingerprint identification system, it is essential to extract fingerprint features. This process consists of three main operations: ridge enhancement, ridge thinning, and minutiae extraction.

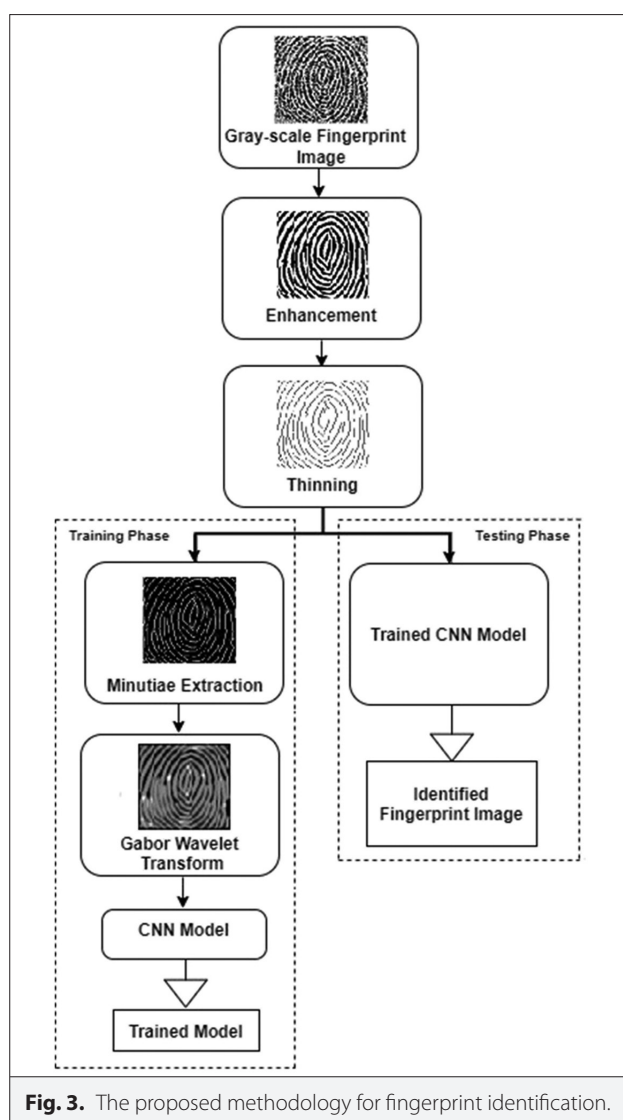


Fig. 3. The proposed methodology for fingerprint identification.

B. Ridge Enhancement

Image enhancement process is needed to obtain the ridges and also to reduce the noise. Enhancement algorithm contains a set of processes that use poor quality fingerprint and output improved quality images. In this study dilation which is a morphological operation expanding the objects in an image I was used [12]. It uses a structuring element e . It is denoted by $I \oplus e$ and adds further pixels to both inside and outside boundaries of the objects in the image.

C. Ridge Thinning

After the enhancement ridge thinning is applied to make the minutiae stage easy to handle, each ridgeline should be converted to one-pixel wide chain. In this study, the thinning method given in [20] is used. First, the black pixels are arranged to one while the white pixels are to zero in an $N \times M$ fingerprint image. We operated the algorithm on all black pixels with their eight neighbors. The neighbors of the pixel

A1 are as in Fig. 4. All pixels are tested sequentially according to the two rule sets described below. If a pixel satisfies the rule set 1, it is set to white. Then rule set 2 is applied and if the pixel satisfies the rule set 2, it is set to white as well. If any pixels are altered either via a rule set 1 or rule set 2, all steps are repeated until none of the image pixels are changed. Here, n_{A1} represents the number of black pixel neighbors of A1. On the other hand, T_{A1} represents the number of transitions from white to black, ($0 \geq 1$) in the sequence A2, A3, A4, A5, A6, A7, A8, A9, A2.

Rule set 1:

- 1) The pixel is black and has eight neighbors.
- 2) $2 \leq n_{A1} \leq 6$.
- 3) $T_{A1} = 1$
- 4) At least one of A2, A4 and A6 is white.
- 5) At least one of A4, A6 and A8 is white.

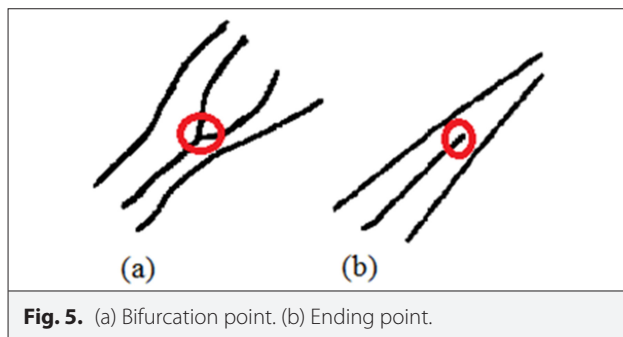
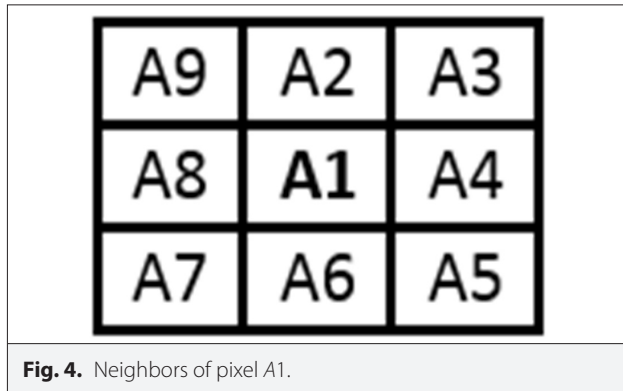
Rule set 2

The first three rules are the same as the rule set 1.

- 1) At least one of A2, A4 and A8 is white.
- 2) At least one of A2, A6 and A8 is white.

D. Minutiae Extraction

The ridge thinning process makes the minutiae detection more accurate and easier. The minutiae points which are the ridge bifurcation and ridge ending points are the most representative features in fingerprint images (Fig. 5). In



this study, the minutiae point P is defined as $P(x,y,l)$ where x and y are the coordinates of the minutiae point. l represents whether the minutiae is a bifurcation or ending point. In the detection algorithm, each fingerprint pixel should be classified as a bifurcation point, ending point, or an ordinary (no-minutiae) point. The no-minutiae points are eliminated and three parameters (x,y,l) for each minutiae point are obtained [21].

The minutiae detection is implemented on binarized and thinned images according to (1) where $l(x,y)$, $l'(x,y)$ and $h(i,j)$ represent the fingerprint pixel of interest, the filtered pixel, and a ones mask of size 3×3 respectively (Figs. 6):

$$l'(x,y) = \sum_{i=-1}^1 \sum_{j=-1}^1 l(x+i,y+j) \cdot h(i,j) \quad (1)$$

$$l = \begin{cases} 0, & l'(x,y) = 2 \\ 1, & l'(x,y) \geq 4 \end{cases}$$

According to (1), the neighbor number is utilized to determine the pixel of interest that is either a bifurcation, an ending, or no-minutiae point. If it is a ridge bifurcation, l is labeled as 1. If it is a ridge ending, l is 0. In these two situations, the x,y coordinates and the corresponding l values are added to $P(x,y,l)$ minutiae set. The pixel of interest is determined as no-minutiae when $l'(x,y) = 3$.

E. Gabor Wavelet Transform

Gabor filters extract both frequency and orientation properties in spatial and frequency domains [22]. Also, wavelet transform produces both the spatial and frequency information of an image considered as multi-resolution time-frequency analysis. The Gabor wavelet transform is a frequently used wavelet transform type. It is efficient in measuring local spatial frequencies due to having multi-resolution and multi-orientation properties. A two-dimensional Gabor function $G(x,y)$ can be defined below as in [23]:

$$G(x,y) = \frac{f^2}{\pi\gamma\eta} \exp\left(-\left(\frac{f^2}{\gamma^2}x_r^2 + \frac{f^2}{\eta^2}y_r^2\right)\right) \exp(j2\pi fx_r) \quad (2)$$

$$x_r = x \cos \theta + y \sin \theta, y_r = -x \sin \theta + y \cos \theta$$

where f is the frequency of the wave, θ is the orientation of the elliptical Gaussian's major axis, and γ and η are the constants. Two-dimensional (2-D) wavelet transform can be written as

$$\Psi_\theta(s_x, s_y, x, y, x_0, y_0) = \frac{1}{\sqrt{s_x s_y}} \Psi_\theta\left(\frac{x-x_0}{s_x} + \frac{y-y_0}{s_y}\right) \quad (3)$$

where $\Psi_\theta(x,y)$ is the mother wavelet which has x_0 and y_0 spatial shifting, θ orientation and s_x and s_y scaling parameters.

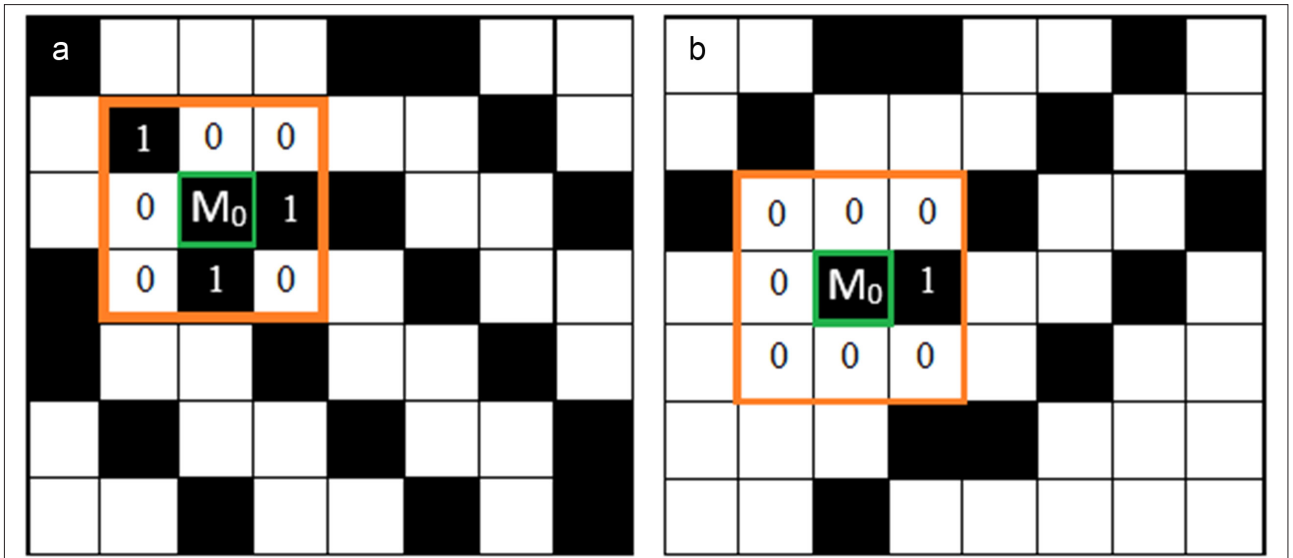


Fig. 6. (a) Bifurcation region neighborhood. (b) Ending region neighborhood.

$G(x,y)$ function can be considered as a set of Gabor wavelets in the presence of real, symmetric, vanishing moments, and admissibility criterion. A magnitude threshold is determined to provide the constraints of being real and symmetric. In (4) $G(x,y)$ can be modified as Gabor wavelet [24] where u, θ and σ represent the frequency of a sinusoidal wave, orientation, and standard deviation of Gaussian function respectively. As Gabor wavelet is complex, (4) produces a complex 2-D signal whose absolute is used in this study to keep the edge features. In Fig. 7 the real part of Gabor wavelets is demonstrated with 4 scales and 4 orientations:

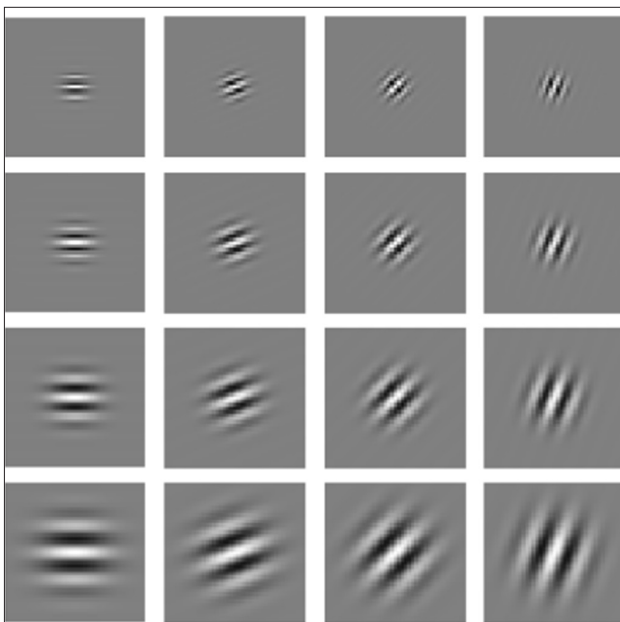


Fig. 7. Real part of Gabor wavelets with 4 scales and 4 orientations.

$$G(x, y, \theta, u, \sigma) = \frac{1}{2\pi\sigma^2} \exp\left\{-\frac{x^2 + y^2}{2\sigma^2}\right\} \exp\{2\pi j(ux \cos \theta + uy \sin \theta)\} \quad (4)$$

F. Convolutional Neural Networks

Convolutional neural networks are a specific type of neural network that mostly comprises convolutional and non-linear layer, pooling layer, flattening layer, and fully connected layer (Fig. 8).

Convolution and non-linearity layer: In this layer, the whole image is scanned and convolved via filters. Each filter produces a feature map that can be smaller than the original image due to not using padding. Feature maps corresponding to different kinds of features are generated as the result of this layer. The features are related to both low-level and higher-level image attributes [25]. The non-linearity layer is also called as ReLu (rectified linear activation function) layer. Rectifier function uses non-linearity with $-f(x) = \max(0,x)$ which converts the negative values to 0.

1) **Pooling layer:**

The aim of this layer is to reduce the spatial size of the feature maps [26]. A maxpooling filter is applied to take the maximum convolution values within a defined neighborhood as seen in Fig. 9.

2) **Flattening layer:**

The flattening layer resides in the classification stage and it prepares the input for the fully connected layer which is the final and most essential layer. In this layer, the data turns into a one-dimensional vector.

3) **Fully connected layer:**

It is the last layer and is responsible for the classification. In this layer, each input is connected to all network

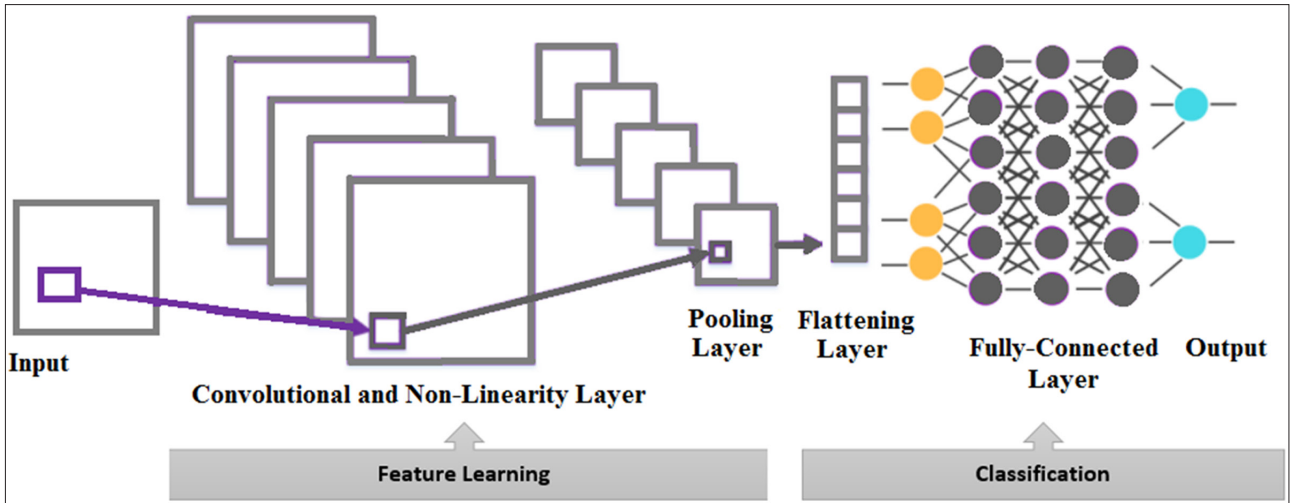


Fig. 8. CNN model.

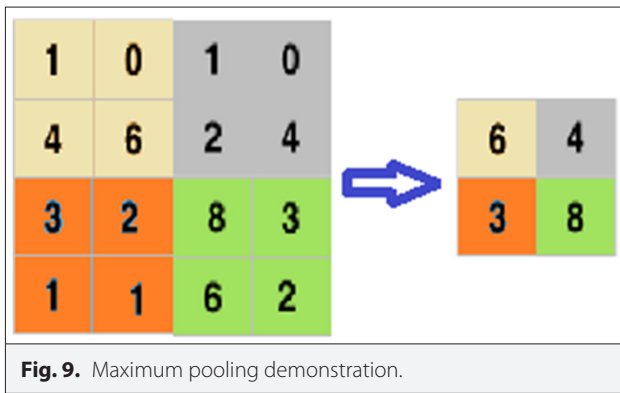


Fig. 9. Maximum pooling demonstration.

neurons. It takes input from the flattening layer and forwards it to the network through training and classification [17].

G. Training Convolutional Neural Network

As known CNNs perform classification by training a related data set. In this study error backpropagation algorithm in which the weights are shared in all layers, is applied in training. The error function E_s is minimized after each training sample s :

$$E_s = \frac{1}{2} O_s - T_s^2 = \frac{1}{2} \sum_{n=1}^N (O_{sn} - T_{sn})^2 \quad (5)$$

where N is the number of output units, O_{sn} is the output of n^{th} neuron of sample s , and T_{sn} is the corresponding target. The training process is iterative and at each iteration, the weights are updated. In (6) Δw , α , and $w_{ji}^{(l)}$ represent the weight change, learning rate, and the weight from i^{th} to j^{th} neuron in layer l [27]:

$$\Delta w_{ij}^{(l)} = -\alpha \delta_n^{(l)} y_j^{(l-1)} \quad (6)$$

In the convolution layer the adjustment of the weight $w_{ji}(u,v)$ from feature map i to j at (u,v) position is a sum of all positions (x,y) of the feature map ((7)):

$$\Delta w_{ji}^{(l)}(u,v) = -\alpha \sum_{(x,y)} (\delta_j^{(l)}(x,y) y_i^{(l-1)}(x+u, y+v)) \quad (7)$$

In (8) δ represents the local gradient in case $l+1$ is a sub-sampling layer. b_x, b_y are sub-sampling factors. $\lfloor \cdot \rfloor$ is the floor function and N_b demonstrates the feature maps in layer $l+1$ connected to j which is the sub-sampling map in l^{th} layer [27]:

$$\delta_j^{(l)}(x,y) = \sum_{n \in N_b} \delta_n^{(l+1)} (\lfloor x/b_x \rfloor, \lfloor y/b_y \rfloor) \cdot w_{nj}^{(l+1)} \quad (8)$$

III. EXPERIMENTAL RESULTS

A. Dataset

FVC2006 dataset was used for the experimentation process. 1680 fingerprint samples of size 96×96 were selected from 140 persons. Four distinct databases are provided by the organizers: DB1, DB2, DB3, and DB4 with the properties given in Table I.

B. Data Augmentation

Image augmentation is a technique of applying different transformations to original images which results in multiple transformed copies of the same image. Applying small amounts of variations on the original image expands the size of the dataset and provides a level of variation in the dataset which makes the model generalize more accurately on unseen data. In this study, we generate different images from original images using 0.1 width shift range, 0.1 height shift range, 0.1 zoom range, and 10 rotation ranges (Fig. 10).

TABLE I. PROPERTIES OF THE DATASET

	Sensor Type	Image Size	Set A (wxd)	Set B (wxd)	Resolution
DB1	Electric field sensor	96×96 (9 Kpixels)	140×12	10×12	250 dpi
DB2	Optical sensor	400×560 (224 Kpixels)	140×12	10×12	569 dpi
DB3	Thermal sweeping sensor	400×500 (200 Kpixels)	140×12	10×12	500 dpi
DB4	SFinGe v3.0	288×384 (108 Kpixels)	140×12	10×12	500 dpi

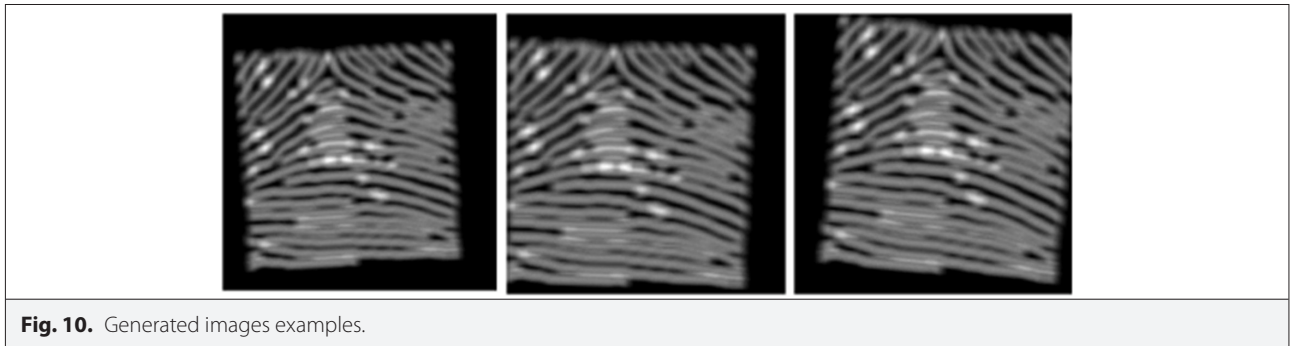


Fig. 10. Generated images examples.

C. Model Evaluation

In the proposed model the gray-scale images were passed through enhancement, thinning, minutiae extraction, and Gabor wavelet transform processes (Fig. 11). And then we

implemented a CNN model which includes three times 2D convolution + pooling layers with different filter parameters, a fully connected layer, and 141 classes in the output layer to identify the fingerprint images as seen in Fig. 12.

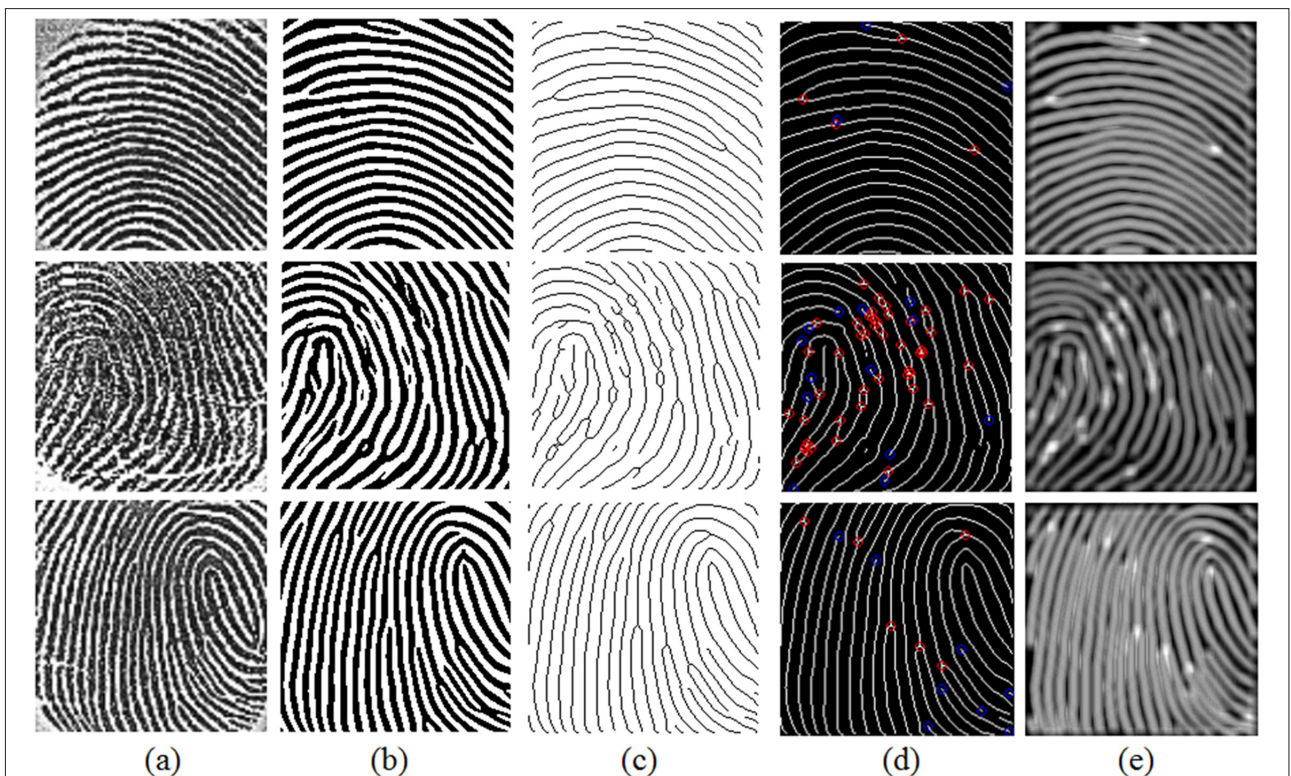


Fig. 11. (a) Gray-scale fingerprint, (b) Enhanced image, (c) Thinned image, (d) Minutiae extraction, (e) The mean GWT applied to the image in (d).

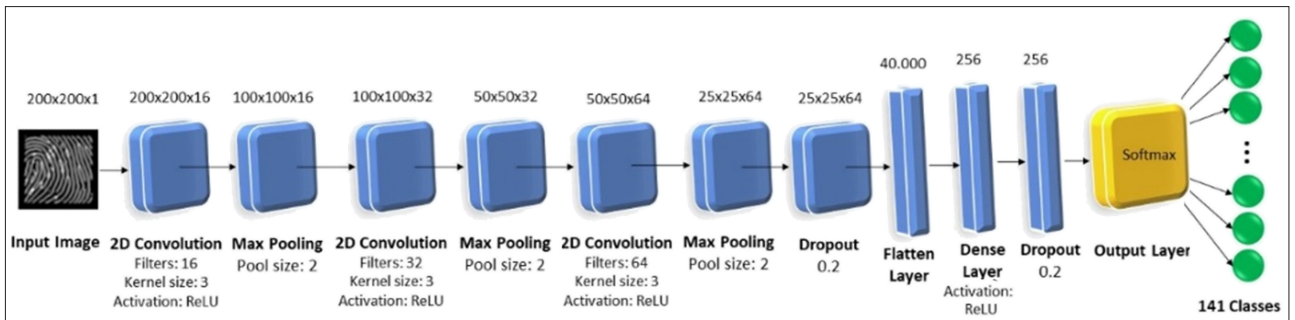


Fig. 12. Proposed CNN architecture model.

We used Adam as an optimizer, categorical cross-entropy as a loss function, and accuracy as a metric during compiling the model. The model was trained in 350 epochs, Figs. 13 and 14 show train and validation accuracy and loss values through iterations respectively.

In the training and testing stages ten-fold cross-validation method was used. Table II demonstrates the performance metrics of the proposed method and the model in which only minutiae extraction was implemented without utilizing GWT to emphasize the effect of the GWT. According to this table, GWT features combined with the minutiae features overcomes the model using only minutiae features with an accuracy of 91.50%, specificity of 99.92%, recall of 91.50%, F1-score of 92.06%, and precision of 94.46% values.

Table III [17,28-31] demonstrates the comparison of fingerprint identification accuracy of our proposed method with existing methods.

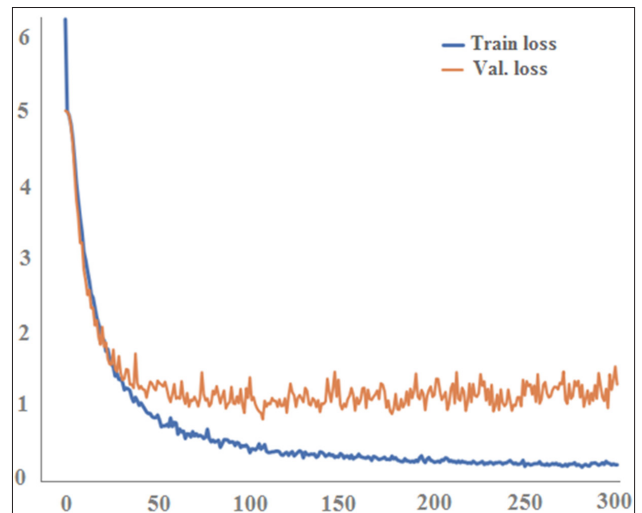


Fig. 14. Train loss/validation loss-iteration graphic.

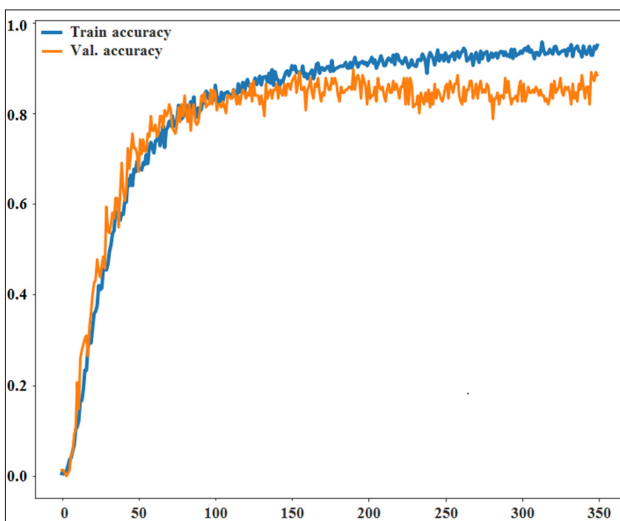


Fig. 13. Train/validation accuracy-iteration graphic.

IV. CONCLUSION

In this work, we implemented an automatic fingerprint identification system using FVC2006 dataset in the training and testing processes. 1680 fingerprint images also including poor quality ones were utilized. As image enhancement affects minutiae detection performance directly, we first implemented the enhancement with dilation morphological operation and thinning sequentially. Moreover, we experienced that using minutiae features only is not enough for a high identification accuracy. Hence, Gabor wavelet transform which helps to acquire both frequency and orientation properties in spatial and frequency domains has been applied to the minutiae extracted images. This process increased the classification accuracy from 86.27% to 91.50%. Also, the system performance is analyzed by recall, precision, F1-score, and specificity metrics. We have constructed our own CNN classification model regarding the problem. Three convolution layers were used with filters of sizes 16, 32, and 64 respectively. Experimental results show the effectiveness of the

TABLE II. PERFORMANCE METRICS

	Acc.(%)	F1-Score (%)	Specificity (%)	Recall (%)	Precision (%)
Minutiae features + CNN	86.27	86.11	99.88	86.27	88.07
Minutiae features + GWT + CNN	91.50	92.06	99.92	91.50	94.46

TABLE III. COMPARISON OF THE IDENTIFICATION ACCURACY OF THE PROPOSED METHOD WITH THE EXISTING METHODS

Author	Method	Accuracy (%)
Kai Cao and Anil K. Jain [17]	Minutiae + CNN	84.10
Sen Wang and Yangsheng Wang [28]	Curvature features + isotropic filters	81.84
Zahra E. Khatab et al. [29]	Autoencoders	87.73
Xuejun Tan and Bir Bhanu [30]	Genetic algorithm	85.00
Miguel A. Medina-Pérez et al. [31]	Minutiae cylinder-codes	85.60
Our Approach	Minutiae + GWT + CNN	91.50

proposed methodology. Further studies will aim to improve the methodology and increase the performance.

Peer-review: Externally peer-reviewed.

Author Contributions: Concept – P.G., A.E.; Design – P.G., A.E.; Supervision – P.G.; Materials – P.G., A.E.; Data Collection and/or Processing – A.E.; Analysis and/or Interpretation – P.G., A.E.; Literature Search – P.G.; Writing Manuscript – P.G., A.E.; Critical Review – P.G.

Conflict of Interest: The authors have no conflicts of interest to declare.

Financial Disclosure: The authors declared that this study has received no financial support.

REFERENCES

- P. Gupta, K. Tiwari and G. Arora, "Fingerprint indexing schemes: A survey," *Neurocomputing*, vol. 335, pp. 352–365, 2019. [\[CrossRef\]](#)
- D. Maltoni, D. Maio, A. K. Jain and S. Prabhakar, *Handbook of Fingerprint Recognition*, London, England: Springer Science and Business Media, 2009.
- S. Dargan and M. Kumar, "A comprehensive survey on the biometric recognition systems based on physiological and behavioral modalities," *Expert Syst. Appl.*, vol. 143, pp. 1–27, 2020. [\[CrossRef\]](#)
- F. Liu, Y. Zhao, G. Liu and L. Shen, "Fingerprint pore matching using deep features," *Pattern Recognit.*, vol. 102, 2020. [\[CrossRef\]](#)
- M. Puertas, D. Ramos, J. Fierrez, J. Ortega-García and N. Exposito, "Towards a better understanding of the performance of latent fingerprint recognition in realistic forensic conditions," 20th International Conference on Pattern Recognition, Istanbul, Turkey, 2010, pp. 1638–1641.
- D. Zhang, F. Liu, Q. Zhao, G. Lu and N. Luo, "Selecting a reference high resolution for fingerprint recognition using minutiae and pores," *IEEE Trans. Instrum. Meas.*, vol. 60, no. 3, pp. 863–871, 2011. [\[CrossRef\]](#)
- J. Zeobiejesi and B. Bhanu, "Latent fingerprint image segmentation using deep neural network," in *Adv. Comput. Vis. Pattern Recognit.*, Berlin: Springer, pp. 83–107, 2017. [\[CrossRef\]](#)
- R. Cappelli, "Fast and accurate fingerprint indexing based on ridge orientation and frequency," *IEEE Trans. Syst. Man Cybern. B Cybern.*, vol. 41, no. 6, pp. 1511–1521, 2011. [\[CrossRef\]](#)
- S. O. Lee, Y. G. Kim and G. T. Park, "A feature map consisting of orientation and inter-ridge spacing for fingerprint retrieval," in *Lecture Notes in Computer Science*. Berlin: Springer, pp. 184–190, 2005. [\[CrossRef\]](#)
- V. Anand and V. Kanhangad, "Pore based indexing for high-resolution fingerprints," *Proceedings of the IEEE International Conference on Identity, Security and Behavior Analysis (ISBA)*, New Delhi, India, 2017, pp. 1–6.
- K. Tiwari and P. Gupta, "Indexing fingerprint database with minutiae based coaxial gaussian track code and quantized lookup table," in *Proceedings of the IEEE International Conference on Image Processing (ICIP)*. IEEE Publications, 2015, pp. 4773–4777.
- U. Jayaraman, A. K. Gupta and P. Gupta, "An efficient minutiae based geometric hashing for fingerprint database," *Neurocomputing*, vol. 137, pp. 115–126, 2014. [\[CrossRef\]](#)
- Z. Jin, A. B. J. Teoh, T. S. Ong and C. Tee, "A revocable fingerprint template for security and privacy preserving," *KSII Trans. Internet Inf. Syst.*, vol. 4, no. 6, pp. 1327–1342, 2010.
- S. Wang and J. Hu, "Alignment-free cancelable fingerprint template design: A densely infinite-to-one mapping approach," *Pattern Recognit.*, vol. 45, no. 12, pp. 4129–4137, 2012. [\[CrossRef\]](#)
- A. Muñoz-Briseño, A. Gago-Alonso and J. Hernández-Palancar, "Using reference point as feature for fingerprint indexing," in *Progress in Pattern Recognition, Image Analysis, Computer Vision and Applications*, E. Bayro-Corrochano, and E. Hancock, Ed. Berlin: Springer, 2014, pp. 367–374.
- K. Cao and A. K. Jain, "Fingerprint indexing and matching: An integrated approach," *IEEE International Joint Conference on Biometrics (IJCB)*, CO, USA, 2017, pp. 437–445.
- K. Cao and A. K. Jain, "Automated latent fingerprint recognition," *IEEE Trans. Pattern Anal. Mach. Intell.*, vol. 41, no. 4, pp. 788–800, 2019. [\[CrossRef\]](#)
- C. C. Bai, W. Q. Wang, T. Zhao, R. X. Wang and M. Q. Li, "Deep learning compact binary codes for fingerprint indexing," *Frontiers Inf. Technol. Electronic Eng.*, vol. 19, no. 9, pp. 1112–1123, 2018. [\[CrossRef\]](#)
- R. Cappelli, M. Ferrara, A. Franco and D. Maltoni, "Fingerprint verification competition 2006," *Biom. Technol. Today*, vol. 15, no. 7–8, pp. 7–9, 2007. [\[CrossRef\]](#)
- K. Karacs, et al., "Software Library for Cellular Wave Computing Engines Version 3.1," *Cellular Sensory and Wave Computing Laboratory of the Computer and Automation Research Inst., Hungarian Academy of Sciences and the Jeddik Laboratories of the Pazmany P. Catholic University*. Budapest, Hungary, 2010.

21. T. Ç. Mayadağlı, E. Saatçi and R. Edizkan, "A CNN based rotation invariant fingerprint recognition system," *IU-JEEE*, vol. 17, no. 2, pp. 3471–3479, 2017.
22. J. G. Daughman, "Uncertainty relation for resolution in space, spatial-Frequency, and orientation optimized by two-dimensional visual cortical filters," *J. Opt. Soc. Am. A*, vol. 2, no. 7, pp. 1160–1169, 1985. [\[CrossRef\]](#)
23. L. Shen and L. Bai, "A review of gabor wavelets for face recognition," *Patt. Anal. Appl.*, vol. 9, pp. 273–292, 2006. [\[CrossRef\]](#)
24. B. Ergen, "A fusion method of gabor wavelet transform and unsupervised clustering algorithms for tissue edge detection," *Sci. World J.*, vol. 2014, pp. 1–13. London, UK: Hindawi Publishing Corporation, 2014.
25. T. J. Su, Y. Y. Du, Y. J. Cheng and Y. H. Su, "A fingerprint recognition system using cellular neural networks," in 9th International Workshop on Cellular Neural Networks and Their Applications. Hsinchu: CNNA, 2005, pp. 170–173.
26. D. Riquelme and M. A. Akhloufi, "Deep learning for lung cancer nodules detection and classification in CT scans," *Artif. Intell.*, vol. 1, no. 1, pp. 28–67, 2020. [\[CrossRef\]](#)
27. S. Duffner, "Face Image Analysis with Convolutional Neural Networks," Doctoral thesis. Germany, Breisgau: The Faculty of Applied Sciences, Albert-Ludwigs University, 2007.
28. S. Wang and Y. Wang, "Fingerprint enhancement in the singular point area," *IEEE Signal Process. Lett.*, vol. 11, no. 1, pp. 16–19, 2004. [\[CrossRef\]](#)
29. Z. E. Khatib, A. H. Gazestani, S. A. Ghorashi and M. Ghavami, "A fingerprint technique for indoor localization using autoencoder based semi-supervised deep extreme learning machine," *Signal Process.*, vol. 181, 2021.
30. X. Tan and B. Bhanu, "Fingerprint matching by genetic algorithms," *Pattern Recognit.*, vol. 39, no. 3, pp. 465–477, 2006. [\[CrossRef\]](#)
31. M. A. Medina-Pérez, A. M. Moreno, M. Á. F. Ballester, M. García-Borroto, O. Loyola-González and L. Altamirano-Robles, "Latent fingerprint identification using deformable minutiae clustering," *Neurocomputing*, vol. 175, pp. 851–865, 2016. [\[CrossRef\]](#)



Pelin Görgel received B.S., M.S., and Ph.D. degrees from Istanbul University, Istanbul, Turkey, in 2003, 2006 and 2011 respectively. She is currently an Assistant Professor at the Department of Computer Engineering, Istanbul University-Cerrahpasa. Her major research interests lie in the areas of artificial intelligence, biomedical image processing, and biometrics.



Abdulsamet Ekşi received B.S. degree from the Gazi University Department of Electrical and Electronics Engineering in 2018. He is currently working at Boni Global inc. as an R&D and Project Development Engineer. His research interests are bioinformatics, image processing, neural networks and machine learning. Currently, he is a graduate student at Istanbul University-Cerrahpasa, Department of Computer Engineering.